ISSN: 2414-1895 DOI: 10.6919/ICJE.202205_8(5).0086

Experimental Study of a Sensor Capable of Increasing the Penetration Depth of Eddy Currents

Chengkai Ye, Siquan Zhang

School of Shanghai Maritime University, Shanghai 201306, China

Abstract

Eddy current inspection methods are widely used in defect detection and non-destructive evaluation of conductive materials. Due to the skinning effect, conventional eddy current inspection methods can only detect shallow locations on the surface of conductors. A new type of phase-shifted field probe has been proposed and experimentally verified to detect defects deeper than the conventional method. An exact theoretical expression for the distribution of eddy currents within a conductor has also been derived from a theoretical perspective. In this paper, the effectiveness of the probe in detecting defects at different depths is investigated in depth from both theoretical and experimental perspectives. It is verified that the probe design and excitation method can indeed change the eddy current density distribution in the conductor and provide better results for deeper defects than the conventional eddy current detection method.

Keywords

Eddy Current Detection; Penetration Depth; Phase-shifted Field Probe; Theoretical Derivation; Experimental Demonstration.

1. Introduction

Non-destructive testing (NDT) technology has developed into an indispensable tool in industry, with applications ranging from aerospace and nuclear power generation to petrochemical, metallurgical and electrical power. The use of effective NDT methods, especially for the detection and quantitative assessment of hidden defects or deep cracks in some large critical components, is important to ensure the operational safety of equipment, assess product life, reduce maintenance costs and avoid serious consequences such as major accidents. Common methods for detecting internal defects or deep cracks include radiographic detection (RT), ultrasonic detection (UT) and alternating current potential drop (ACPD), but they all have certain drawbacks and cannot be widely applied to the rapid online quantitative detection of large components.[1] Eddy current inspection (ECT) is a method that is used to measure the quality of the components. Eddy current inspection (ECT) is a non-destructive testing method applied to conductive materials. It has many advantages such as high sensitivity, fast scanning speed, non-contact detection and versatility, and is therefore widely used. Due to the skin effect, the defect signal saturates as the depth of the defect increases. It is therefore quite difficult to evaluate deep defects when the defect depth exceeds a certain value. In general, lower frequency excitation provides deeper eddy current penetration, however, very low frequency driving poses additional problems[2].

To overcome this difficulty, scholars have tried various methods to increase the penetration depth of eddy currents to detect deep cracks. noritaka Yusa proposed to achieve a unique AC distribution by superimposing several current distributions. l Janousek[4] The use of multiple probes to examine detected cracks, linear superposition of the crack signals and extraction of a unique eigenvalue of the superposition ratio from the resulting signal was proposed by Dongli Zhang[1] A new probe consisting of three circular coils using a phase-shifted field excitation system was proposed.[5] A

ISSN: 2414-1895 DOI: 10.6919/ICJE.202205_8(5).0086

new type of eddy current probe using a solenoidal coil as the excitation source is presented.[2] Ladislav Janousek proposed a new eddy current probe consisting of four coaxial rectangular tangential excitation coils and a pick-up coil, using a phase-shifted field excitation system, the four excitation coils are divided into two groups, the number of turns and the excitation method can be varied by different wiring methods, which can effectively improve the penetration depth. This research is based on the theoretical and experimental study of the method proposed by this scholar.

2. Theoretical Analysis

2.1 Model Analysis

Figure 1(a) shows a single-turn rectangular coil located above a multilayer conductive plate. The surface of the conducting plate coincides with the z=0 plane. The rectangular coil is parallel to the x and z axes and perpendicular to the y axis, with sides of length $2a_0$ and $2b_0$ The distance between the plane in which the coil is located and the z-axis is c. The distance of the centre of the coil from the surface of the conductor is z_0 . A sinusoidal excitation current is passed through the coil $Ie^{j\omega t}$ and I is the current amplitude and ω is the angular frequency. The conductor is a linear, homogeneous and isotropic material. Assume that the thickness, conductivity and permeability of the upper conductor are d, respectively μ_1 and σ_1 and the conductivity and permeability of the lower conductor are μ_2 and σ_2 and the thickness is infinite. Figure 1(b) shows a multi-turn coil formed by extending the single-turn rectangular coil of Figure 1(a) by h/2 in each of the positive and negative directions of the y-axis and by w outwards along all four sides.

For the purposes of this analysis, the entire space has been divided into three zones:

region0: in the z>0 range, there is both the incident flux density from the excitation current B_i and the reflected flux density from induced eddy currents in the conductor B_r.

region1: in the range -d<z<0, is the upper conductive flat plate, where the magnetic flux density existsB_1.

region2: in the z<-d range, which is the lower conductor region, there is a magnetic flux densityB_2[6].

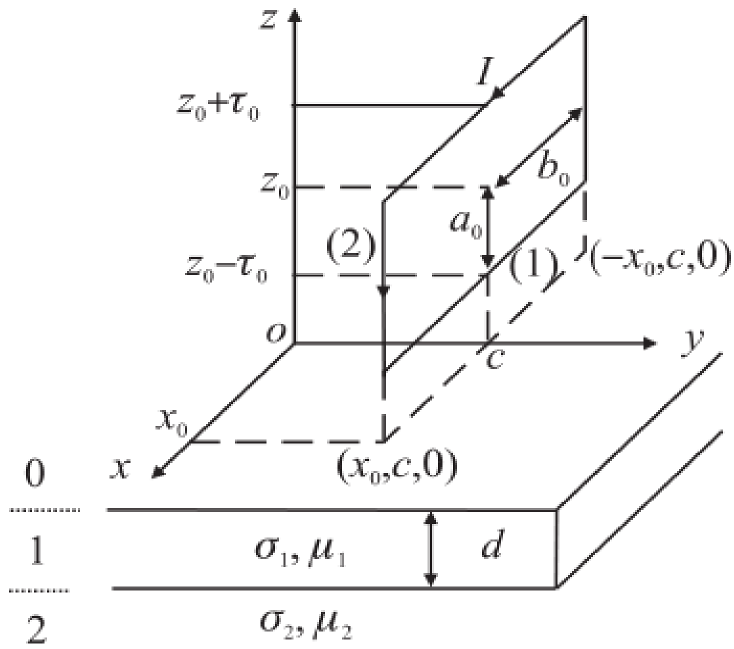

(a) Single-turn rectangular coils

ISSN: 2414-1895 DOI: 10.6919/ICJE.202205_8(5).0086

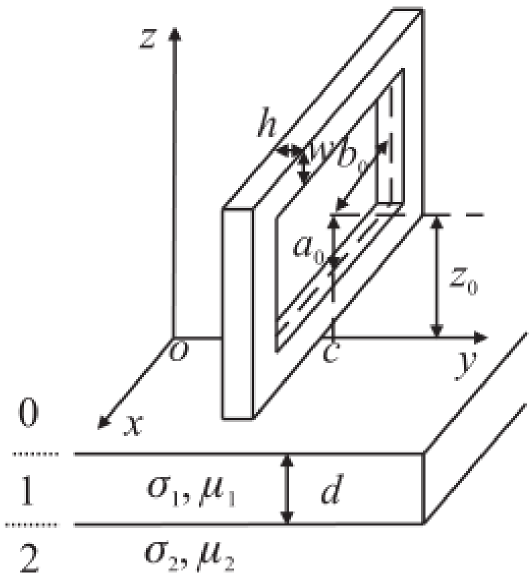

(b) Multi-turn rectangular coils

Figure 1. Rectangular coil above a multilayer conductor

2.2 Coil with In-phase Excitation Current Applied to the Internal and External Coils

A multi-turn coil in figure 1(b) is expanded into an identical multi-turn rectangular coil to form the phase-shifted field probe excitation system shown in figure 2 (b). The four rectangular excitation coils are numbered 1, 2, 3,4 where coil 1, 4 is called the external coil and coil 2,3 is called the internal coil. Let the centres of the four coils correspond to the positions on the y-axis asc_1 , ,c_2 , ,c_3 , , andc_4 .

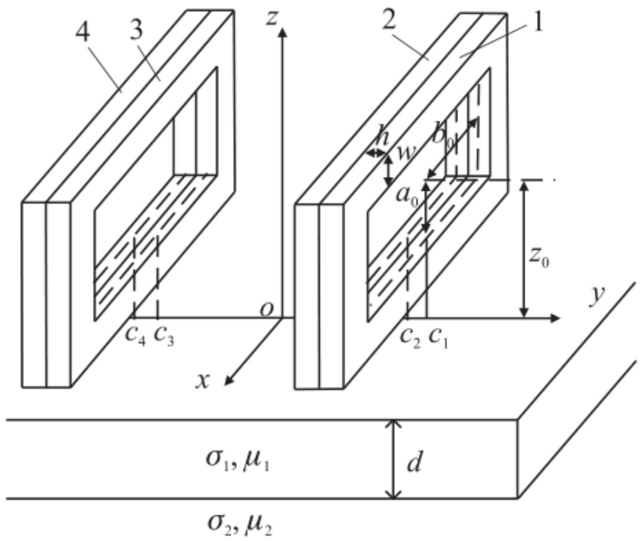

Figure 2. Four multi-turn rectangular excitation coils forming a phase-shifted field probe[6]

Reference to previous literature[7][8].An excitation current of the same direction and phase is applied to the external coil 1,4 while the same excitation current is applied to the internal coil 2,3 as to the external coil. With such an excitation, the phase-shifted field probe is equivalent to a conventional eddy current probe. At this point, the total eddy current density in the conductor is:

$$J_1 = \sqrt{J_x^2 + J_y^2} \tag{1}$$

ISSN: 2414-1895 DOI: 10.6919/ICJE.202205_8(5).0086

where the x and y components of the eddy current are the superposition of the eddy currents produced by four rectangular coils of the same excitation current.

$$J_x = J_{1x} + J_{2x} + J_{3x} + J_{4x} = \frac{-I}{\pi^2 \omega h \mu_r}$$
$$\int_{-\infty}^{\infty}\int_{-\infty}^{\infty}\left(1-\frac{\gamma_1^2}{\varsigma^2}\right)\frac{\eta k_0 k_2}{\xi\varsigma}\left(N_1 e^{j\eta c_1} + N_2 e^{j\eta c_2} + N_3 e^{j\eta c_3} + N_4 e^{j\eta c_4}\right)$$
$$\mathrm{Sin}(\frac{\eta h}{2})(e^{-\gamma_1 z} + \mathrm{P} e^{\gamma_1(2d+z)})e^{-z_0\varsigma}e^{-j(x\xi+y\eta)}d\xi d\eta \quad (2)$$

$$J_y = J_{1y} + J_{2y} + J_{3y} + J_{4y} = \frac{-I}{\pi^2 \omega h \mu_r}$$
$$\int_{-\infty}^{\infty}\int_{-\infty}^{\infty}\left(\frac{\gamma_1^2}{\varsigma^2}-1\right)\frac{k_0 k_2}{\varsigma}\left(N_1 e^{j\eta c_1} + N_2 e^{j\eta c_2} + N_3 e^{j\eta c_3} + N_4 e^{j\eta c_4}\right)$$
$$\mathrm{Sin}(\frac{\eta h}{2})(e^{-\gamma_1 z} + \mathrm{P} e^{\gamma_1(2d+z)})e^{-z_0\varsigma}e^{-j(x\xi+y\eta)}d\xi d\eta \quad (3)$$

2.3 Inverted Excitation Current Applied to the Internal and External Coils

An excitation current in the same direction is applied to the external coil 1,4 and an excitation current in the opposite direction to the external coil is applied to the internal coil 2,3. At this point, the total eddy current density in the conductor is:

$$J_2 = \sqrt{J_x^2 + J_y^2} \quad (4)$$

where the x and y components of the eddy currents are superimposed on the eddy currents generated by the internal and external coils when excited by currents in different directions.

$$J_x = J_{1x} + J_{2x} + J_{3x} + J_{4x} = \frac{-I}{\pi^2 \omega h \mu_r}$$
$$\int_{-\infty}^{\infty}\int_{-\infty}^{\infty}\left(1-\frac{\gamma_1^2}{\varsigma^2}\right)\frac{\eta k_0 k_2}{\xi\varsigma}\left(N_1 e^{j\eta c_1} - N_2 e^{j\eta c_2} - N_3 e^{j\eta c_3} + N_4 e^{j\eta c_4}\right)$$
$$\mathrm{Sin}(\frac{\eta h}{2})(e^{-\gamma_1 z} + \mathrm{P} e^{\gamma_1(2d+z)})e^{-z_0\varsigma}e^{-j(x\xi+y\eta)}d\xi d\eta \quad (5)$$

$$J_y = J_{1y} + J_{2y} + J_{3y} + J_{4y} = \frac{-I}{\pi^2 \omega h \mu_r}$$
$$\int_{-\infty}^{\infty}\int_{-\infty}^{\infty}\left(\frac{\gamma_1^2}{\varsigma^2}-1\right)\frac{k_0 k_2}{\varsigma}\left(N_1 e^{j\eta c_1} - N_2 e^{j\eta c_2} - N_3 e^{j\eta c_3} + N_4 e^{j\eta c_4}\right)$$
$$\mathrm{Sin}(\frac{\eta h}{2})(e^{-\gamma_1 z} + \mathrm{P} e^{\gamma_1(2d+z)})e^{-z_0\varsigma}e^{-j(x\xi+y\eta)}d\xi d\eta \quad (6)$$

Volume 8 Issue 5, 2022
DOI: 10.6919/ICJE.202205_8(5).0086

3. Probe Design

The layout of the excitation system proposed by Ladislav Janousek is shown in the figure 3, with four identical coaxial rectangular coils and internal coils each connected in series to obtain a balance at the centre of the system, with a pick-up coil at the bottom to induce the value of the voltage variations. The internal and external coils are driven by AC currents with different phases and amplitudes. In order to achieve eddy current density suppression on the surface of the specimen under the centre of the excitation system at a specific frequency, the following variables must be correctly adjusted: the spacing s between the excitation groups, the phase of the excitation current in the internal and external coil s, and the number of turns (excitation current density).

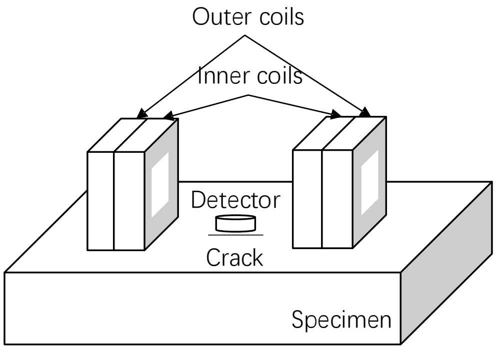

Figure 3. Layout of the excitation system

Eddy current suppression can be achieved on the specimen surface by correct adjustment of the excitation coil. The external coil is driven by a current, phase shifted 180°, with the excitation current of the internal coil. It has been found experimentally that eddy current penetration is greatly improved when the excitation groups are spaced up to50 mm apart. Larger distances between the excitation coil groups reduce the eddy current density and thus the pick-up signal. The ratio between the drive current density of the internal and external coils (the ratio between the number of turns of the internal and external coils) is 0.655 such that the excitation field is phase shifted to obtain the required behaviour for surface eddy current suppression. The configuration and dimensions of the probe are shown in the figure 4.

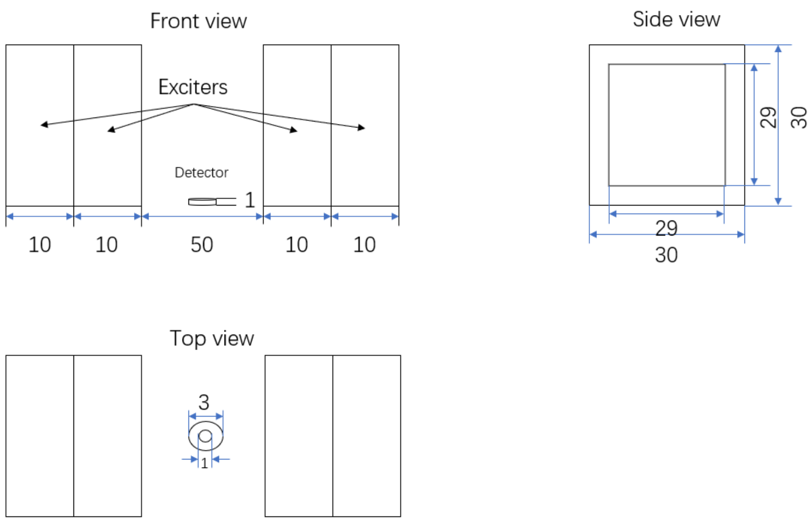

Figure 4. Probe configuration and dimensions

ISSN: 2414-1895
DOI: 10.6919/ICJE.202205_8(5).0086

4. Ansys Simulation Verification

Japanese scholars designed the size of the probe, made a physical object, and set up the experimental platform, through the experimental data analysis of the new probe in improving the effect of eddy current penetration depth. This paper verifies the excellent performance of the new probe from three aspects of theory, simulation and experiment.

4.1 The Establishment of Simulation Model

The 3D model of the excitation system is shown in Figure 5, and the parameters of the model are shown in Table 1.

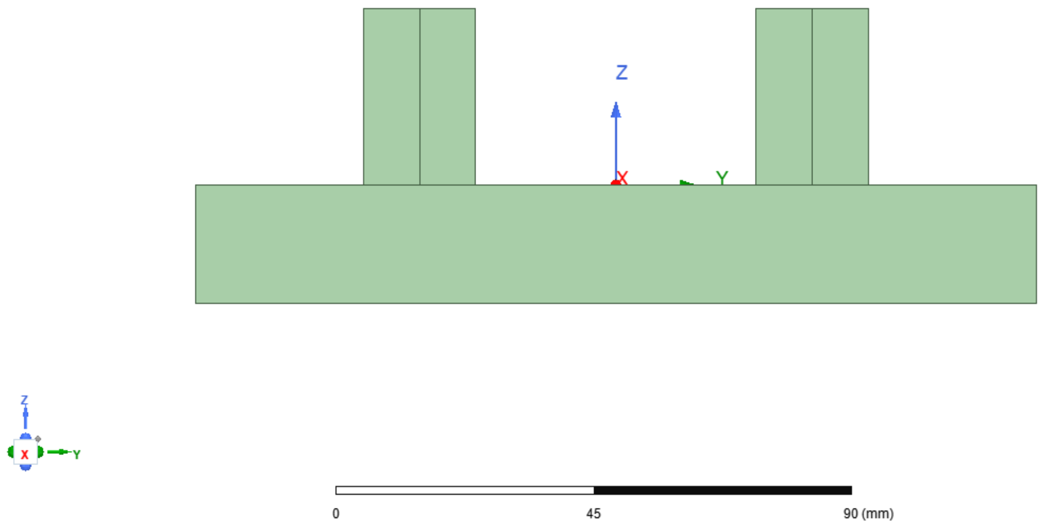

Figure 5. The 3D model of the excitation system

Table 1. Model Parameter List

Parameter	Number
Number of turns of external coil	200
Number of turns of internal coil	120
Conductor plate thickness	20
Conductor plate length	100
Conductor plate width	150
Conductor plate material	Aluminum

4.2 The Simulation Results

In order to more intuitively compare the difference between current and phase shift, the magnetic induction intensity distribution diagram is introduced, as shown in figure 6 and figure 7.

ISSN: 2414-1895
DOI: 10.6919/ICJE.202205_8(5).0086

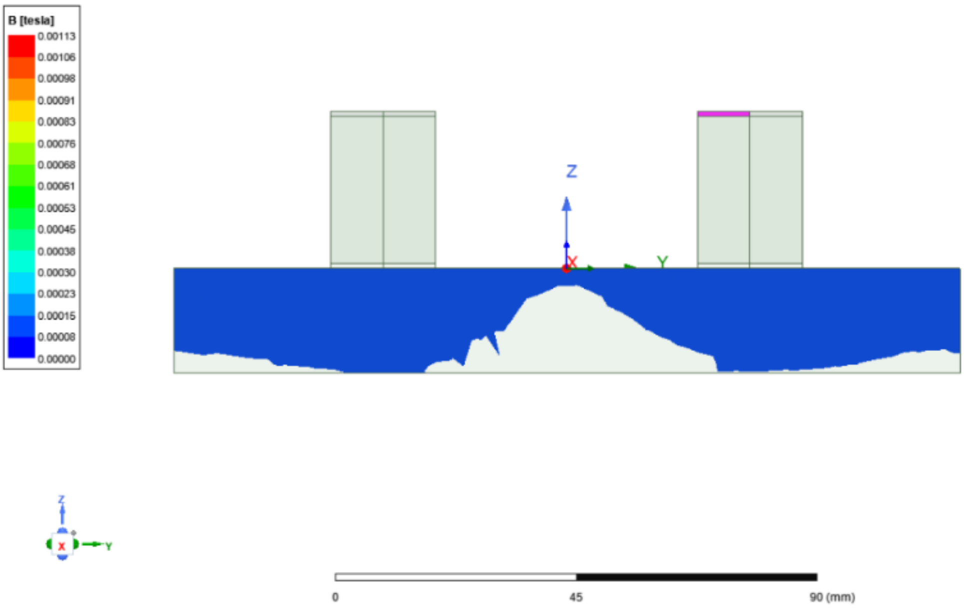

Figure 6. Internal coil current phase shift 180° magnetic induction intensity

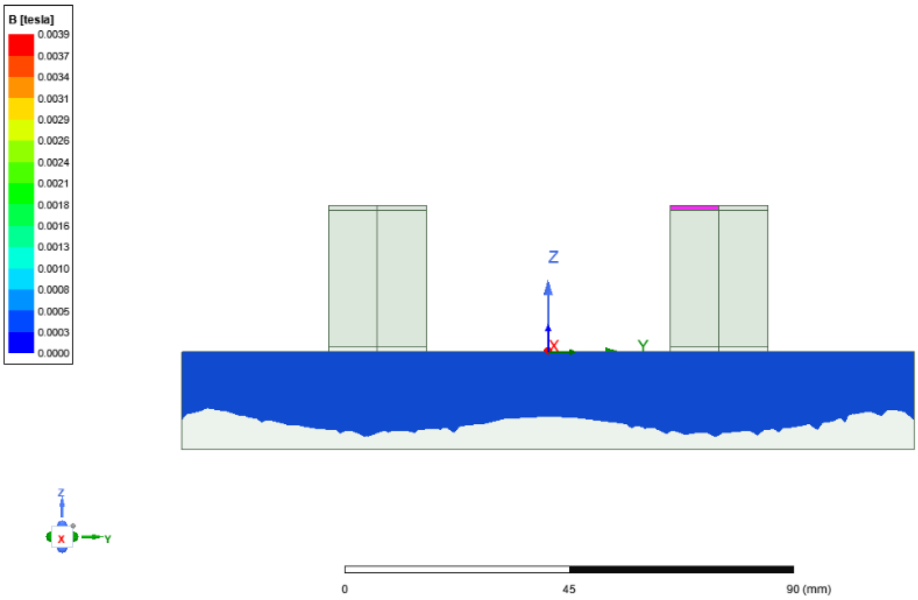

Figure 7. The magnetic induction intensity of the internal coil current without phase shift

From the above figure it can be seen that the depth of eddy current penetration is deeper after a phase shift of 180°, while the surface eddy current is suppressed by the excitation coils on either side. To make the results more convincing, the value of the eddy current density at the origin is derived, as shown in Figure 8 and Figure 9.

	Freq [kHz]	Mag_J [uA_per_m2] Setup1 : LastAdaptive Phase='0deg'
1	10.000000	0.004108

Figure 8. Eddy current density at the origin when the internal coil current is shifted 180° in phase

ISSN: 2414-1895 DOI: 10.6919/ICJE.202205_8(5).0086

	Freq [kHz]	Mag_J [uA_per_m2] Setup1 : LastAdaptive Phase='0deg'
1	10.000000	0.005990

Figure 9. Eddy current density at the origin when there is no phase shift in the internal coil

The graph above shows that the eddy current density at the origin after the current has been phase-shifted by 180° is smaller than without the phase shift, suppressing eddy currents at the surface of the specimen and thus achieving a deeper penetration depth.

5. Experimental Results

5.1 Construction of the Experimental Platform

The experimental platform is shown in Figure 10. The signal generator AFG3021C from Tektronix was used for excitation, set up with parameters and then amplified by a power amplifier from Antec. The signal was picked up and measured using an accurate voltammeter. The necessary data was recorded manually to facilitate analysis. The probe was made from a resin material selected through 3d printing technology, and the completed probe is shown in Figure 11.

The number of turns of the coil, the lift-off height, the frequency, amplitude and magnification of the excitation signal all have an effect on the results of the experiment[9]. In order to investigate how these parameters affect the results, two simple circular coils were made, one as an induction coil and one as a pick-up coil. The results show that the higher the number of turns, the higher the density of eddy currents and the more pronounced the results; the higher the lift-off height, the weaker the induced voltage; the effect of frequency on the induced voltage increases exponentially and the deeper the crack, the greater the variation, the effect of voltage amplitude on the results increases linearly.

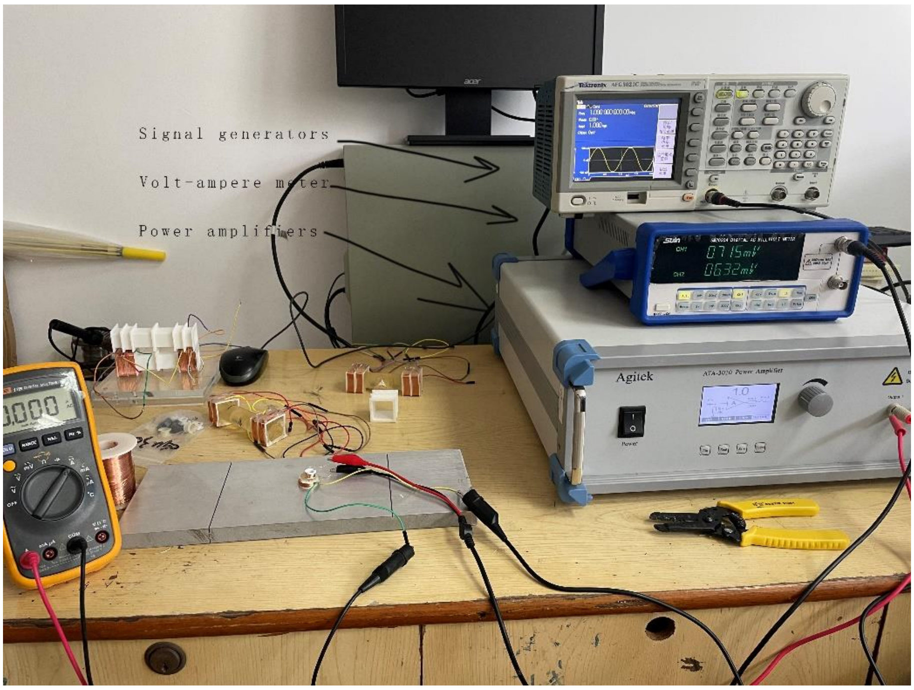

Figure 10. Experimental platform

DOI: 10.6919/ICJE.202205_8(5).0086

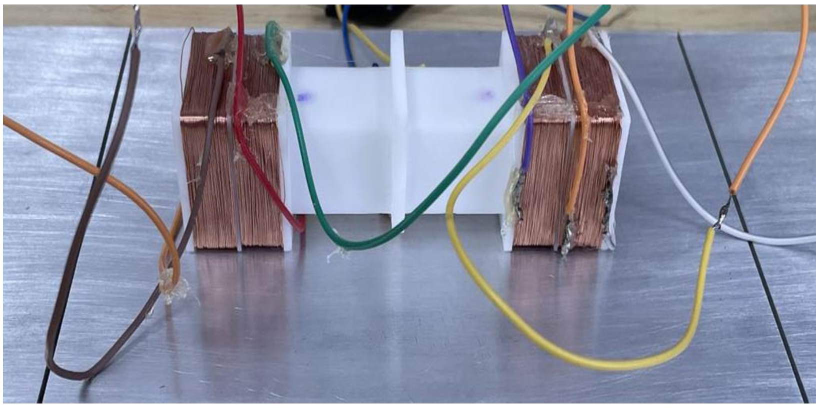

Figure 11. The completed coil

5.2 Experimental Results

The experiment is mainly to compare the performance of conventional eddy current sensor and phase shift eddy current sensor under deep crack, the number of turns of external coil is taken as 200 turns, the internal coil is taken as 120 turns, the amplitude is taken as 1v, the amplification is set as 5 times, by adjusting the frequency, to obtain the induced voltage of the sensor in air, on a 2mm crack and on a 4mm crack, the induced voltage on the crack minus the induced voltage in air is what the crack induced voltage change. The experimental results are shown in Figure 12 and Figure 13.

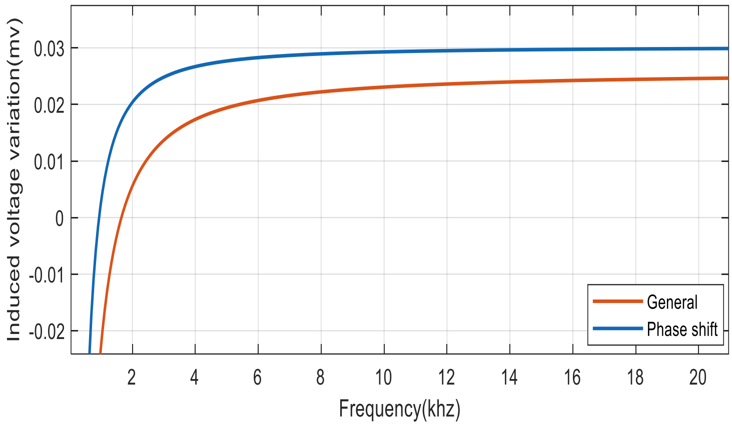

Figure 12. Signal versus frequency for conventional and phase-shifted field probes in the detection of 2mm cracks

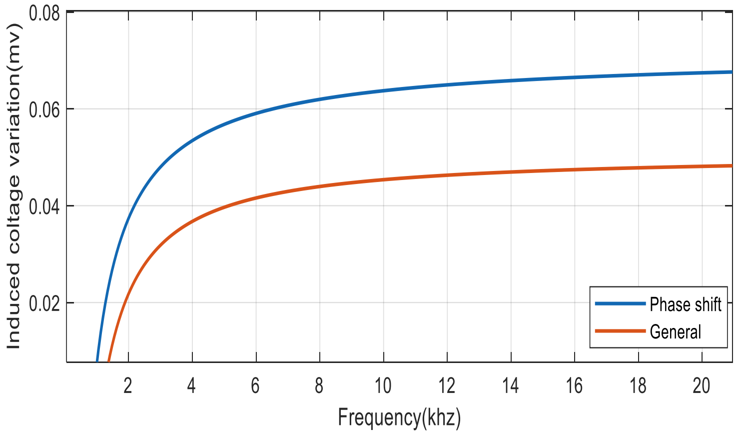

Figure 13. Signal versus frequency for conventional and phase-shifted field probes in the detection of 4mm cracks

ISSN: 2414-1895 DOI: 10.6919/ICJE.202205_8(5).0086

The images above show the performance of conventional eddy current probes and phase shift field probes at different frequencies for different depths of cracks. It can be seen that sensors using phase shift excitation at 1-20khz are significantly better at detecting defects than conventional coils, and also have more pronounced results for deeper eddy currents. At higher frequencies, on the other hand, the phase shift probe does not perform as well as the conventional probe, and perhaps deeper cracks will perform better, requiring more experimental demonstration.

6. Conclusion

This paper verifies that the method is indeed effective in improving the limitations of conventional eddy current sensors with better performance in deeper cracks, based on a new sensor design idea proposed by scholars from theory, simulation and experiment. The main innovation of the probe is the use of a phase-shifted field excitation, consisting of four coaxial tangential rectangular coils forming two separated excitation groups. The external and internal sensors are connected in series to ensure balance at the centre of the probe where the pick-up coils are located and to enable phase shifted excitation. Better detection is achieved by correctly adjusting the spacing between the two excitation groups and the excitation current density with opposite phases. The general performance of the new probe has yet to be verified in more detailed experiments to demonstrate its general applicability in different situations.

Acknowledgments

Upon the completion of this thesis, I would like to express my sincere thanks to my classmates, teachers and family members for their care and help.

References

[1] Zhang D , Wu M , Wang C . A Novel Deep Penetrating Eddy Current Probe for Inspection of Deep Cracks in SUS304[C]// 2019 International Conference on Sensing, Diagnostics, Prognostics, and Control (SDPC). 2019.

[2] Janousek L , Chen Z , Yusa N . Excitation with phase shifted fields-enhancing evaluation of deep cracks in eddy-current testing[J]. Ndt & E International, 2005, 38(6):508-515.

[3] Yusa N , Janousek L , Miya K . Controlling Alternating Current Distribution inside Conductive Material Leads to a Novel Volumetric Examination Method -Experimental Verification[J]. Materials Transactions, 2007, 48(6):1162-1165.

[4] Janouek L , D Gombárska, K ￼ová. A new approach for enhancing eddy-current non-destructive evaluation[J]. Západočeská Univerzita, 2007.

[5] Wu M , Zhang D , Zhou C . A New Eddy Current Probe for Inspection of Deep Delamination Defects Using a Solenoid-Coil Exciter[C]// 2019 International Conference on Sensing, Diagnostics, Prognostics, and Control (SDPC). IEEE, 2019.

[6] Zhang SQ, Tang JF. Theoretical validation of a novel phase-shifted field probe to change eddy current distribution in conductors[J]. Journal of Sensing Technology,2016,29(08):1169-1175.

[7] Zhang S , Nathan I , Wu W . Thickness measurement of metal coating above moving conductive plate by rectangular coil and electromagnetic method[C]// IEEE International Conference on Electronic Measurement & Instruments. IEEE, 2016.

[8] Zhang S , Tang J , Wu W . Calculation model for the induced voltage of pick-up coil excited by rectangular coil above conductive plate[C]// IEEE International Conference on Mechatronics & Automation. IEEE, 2015:1805-1810.

[9] Janousek L . Impact of selected parameters on eddy current attenuation in conductive materials[C]// 2012 ELEKTRO. IEEE, 2012.